Zeki ŞAHBAZ

M.Sc. Thesis

AGU 2024

TUMOR DETECTION IN BREAST CANCER HISTOPATHOLOGICAL IMAGES USING CONVOLUTIONAL NEURAL NETWORKS

M.Sc. THESIS
SUBMITTED TO THE DEPARTMENT OF ELECTRICAL AND COMPUTER ENGINEERING
AND THE GRADUATE SCHOOL OF ENGINEERING AND SCIENCE
OF ABDULLAH GUL UNIVERSITY
IN PARTIAL FULFILLMENT OF THE REQUIREMENTS
FOR THE DEGREE OF
MASTER OF SCIENCE

By
Zeki ŞAHBAZ
May 2024

TUMOR DETECTION IN BREAST CANCER HISTOPATHOLOGICAL IMAGES USING CONVOLUTIONAL NEURAL NETWORKS

A THESIS
SUBMITTED TO THE DEPARTMENT OF ELECTRICAL AND COMPUTER ENGINEERING
AND THE GRADUATE SCHOOL OF ENGINEERING AND SCIENCE OF ABDULLAH GUL UNIVERSITY
IN PARTIAL FULFILLMENT OF THE REQUIREMENTS
FOR THE DEGREE OF
MASTER OF SCIENCE

By
Zeki ŞAHBAZ
May 2024

SCIENTIFIC ETHICS COMPLIANCE

I hereby declare that all information in this document has been obtained in accordance with academic rules and ethical conduct. I also declare that, as required by these rules and conduct, I have fully cited and referenced all materials and results that are not original to this work.

Name-Surname: Zeki ŞAHBAZ
Signature :

REGULATORY COMPLIANCE

M.Sc. thesis titled **"TUMOR DETECTION IN BREAST CANCER HISTOPATHOLOGICAL IMAGES USING CONVOLUTIONAL NEURAL NETWORKS"** has been prepared in accordance with the Thesis Writing Guidelines of the Abdullah Gül University, Graduate School of Engineering & Science.

Prepared By	Advisor
Zeki ŞAHBAZ	Assist. Prof. Bekir Hakan AKSEBZECİ

Head of the Electrical and Computer Engineering Graduate Program
Assist. Prof. Samet GÜLER

ACCEPTANCE AND APPROVAL

M.Sc. thesis titled **"TUMOR DETECTION IN BREAST CANCER HISTOPATHOLOGICAL IMAGES USING CONVOLUTIONAL NEURAL NETWORKS"** and prepared by Zeki SAHBAZ has been accepted by the jury in the Electrical and Computer Engineering Graduate Program at Abdullah Gül University, Graduate School of Engineering & Science.

31/05/2024

JURY:

Advisor : Assist. Prof. Bekir Hakan AKSEBZECİ

Member : Assoc. Prof. Rifat KURBAN

Member : Assist. Prof. Ahmet Nusret TOPRAK

APPROVAL:

The acceptance of this M.Sc. thesis has been approved by the decision of the Abdullah Gül University, Graduate School of Engineering & Science, Executive Board dated ….. /….. / …….. and numbered ……..……. .

…….. /…….. / ……..

(Date)

Graduate School Dean
Prof. İrfan ALAN

ABSTRACT

TUMOR DETECTION IN BREAST CANCER HISTOPATHOLOGICAL IMAGES USING CONVOLUTIONAL NEURAL NETWORKS

Zeki ŞAHBAZ
MSc. in Electrical and Computer Engineering
Advisor: Assist. Prof. Bekir Hakan AKSEBZECİ
May 2024

Breast cancer is one of the most common cancer types among women worldwide. Early detection significantly increases the chances of survival and effective treatment, making advancements in diagnostic methodologies crucial. This study aims to improve the detection of tumor cells in breast cancer histopathology images using deep learning and image processing techniques. Significant modifications have been made to the hyperparameters, including the tumor bounding box size, batch size, optimization algorithms, learning rate, and weight decay. These changes focus on determining the best parameters of the Faster R-CNN model. A comprehensive analysis of different parameters was conducted using the Breast Cancer Histopathological Annotation and Diagnosis (BreCaHAD) dataset. The analysis identified the best settings for model performance, shows by improvements in precision, recall, and F-score. Our research contributes to the field of medical image analysis by identifying critical factors that affect the accuracy of tumor detection, contributing to the development of more accurate diagnostic tools.

Keywords: Breast Cancer, Histopathological Images, Deep Learning, Convolutional Neural Networks, Tumor Detection

ÖZET

MEME KANSERİ HİSTOPATOLOJİ GÖRÜNTÜLERİNDE EVRİŞİMSEL SİNİR AĞLARI KULLANARAK TÜMÖR TESPİTİ

Zeki ŞAHBAZ
Elektrik ve Bilgisayar Mühendisliği Anabilim Dalı Yüksek Lisans
Tez Danışmanı: Dr. Öğr. Üyesi Bekir Hakan AKSEBZECİ
Mayıs 2024

Meme kanseri, dünya genelinde kadınlar arasında görülen en yaygın kanser türlerinden biridir. Erken teşhis konulduğu zaman, hayatta kalma ve tedavi ihtimali arttığı için tanı metodolojilerindeki gelişmeler önemlidir. Bu çalışma, derin öğrenme ve görüntü işleme tekniklerini kullanarak meme kanseri histopatoloji görüntülerindeki tümör hücrelerinin tespitinde iyileştirme yapmayı hedeflemektedir. Özellikle tümör çevresini kapsayan kutuların boyutu, aynı andaki toplu iş sayısı, optimizasyon algoritmaları ve öğrenme hızı ile ağırlık azaltma dahil olmak üzere hiperparametrelerde farklı değerler sınanmaktadır. Bu değişkenler ile Faster R-CNN modelinin iyileştirilmesine odaklanılmaktadır. Meme Kanseri Histopatoloji Anotasyon ve Tanı (BreCaHAD) veri setini kullanarak çeşitli parametrelerde geniş bir analiz yapılmıştır. Analiz sonucunda, model performansını artıran en iyi parametreler belirlenerek; hassasiyet, geri çağırma ve F-skoru gibi önemli metriklerde iyileşme sağlanmıştır. Meme kanseri histopatoloji görüntülerinde tümör tespiti doğruluğunu etkileyen kritik faktörleri kapsamlı bir şekilde inceleyen bu çalışma, tıbbi görüntü analizi alanına önemli katkılar sunmaktadır. Elde edilen sonuçlar, daha güvenilir ve doğru tanıya katkıda bulunabilecek yeni araştırma alanları ve geliştirme yolları için sağlam bir temel oluşturmaktadır.

Anahtar kelimeler: Meme Kanseri, Histopatolojik Görüntüler, Derin Öğrenme, Evrişimsel Sinir Ağları, Tümör Tespiti

Acknowledgements

i. I want to say my gratitude to my supervisor, Assistant Professor Bekir Hakan AKSEBZECİ, for his guidance and support throughout this research. His knowledge and motivational encouragement contributed to the successful completion of this thesis.
ii. I also express my gratitude to Associate Professor Rifat KURBAN and Assistant Professor Ahmet Nusret TOPRAK for serving on my dissertation defense committee. Additionally, I would like to thank Assistant Professor Fehim KÖYLÜ for his guidance.
iii. I deeply appreciate my wife for their valuable support, sacrifices and confidence in my capabilities. My heartfelt thanks also go out to my little Mete.

TABLE OF CONTENTS

1. INTRODUCTION 1

2. LITERATURE REVIEW 4

3. MATERIALS AND METHODS 7

3.1 DATASET 8
3.2 ALGORITHM 9
3.3 IMAGE PROCESSING 11
3.4 FASTER R-CNN 12
3.5 OPTIMIZER 14
3.6 PARAMETER OPTIMIZATION 15

4. EXPERIMENTAL RESULTS 16

4.1 ENVIRONMENTAL SETUP 17
4.2 PERFORMANCE EVALUATION METRICS 17
4.2.1 Intersection over Union (IoU) 17
4.2.2 Precision and Recall 18
4.2.3 F-score 18
4.3 PROPOSED METHOD 18
4.3.1 Configuration Parameters of Proposed Method 19
4.3.2 Data Splitting 20
4.3.3 Image Processing 20
4.3.4 Model Training 20
4.3.5 Test Model 21
4.4 OPTIMIZING PARAMETERS 21
4.5 BACKBONE BENCHMARKS 24
4.6 FINDING THE OPTIMAL IMAGE PROCESSING 25
4.7 WEIGHT DECAY OPTIMIZATION 27

5. CONCLUSIONS AND FUTURE PROSPECTS 28

5.1 CONCLUSIONS 28
5.2 SOCIETAL IMPACT AND CONTRIBUTION TO GLOBAL SUSTAINABILITY 29
5.3 FUTURE PROSPECTS 30

LIST OF FIGURES

Figure 3.1 General structure of our proposed method 7
Figure 3.2 Original images and annotated images 9
Figure 3.3 Faster R-CNN architecture 13
Figure 4.1 Original image vs predicted boxes image 19
Figure 4.2 Epoch vs learning rate 24
Figure 4.3 Applied image processing techniques 26

LIST OF TABLES

Table 2.1 F-score comparisons of images by using normalization technique 4
Table 2.2 Comparison object detection models 5
Table 3.1 Distribution of cell types by annotation colors 8
Table 4.1 Parameters and tested values 19
Table 4.2 Results of combinations: Box Size, optimizer, batch size, learning rate 22
Table 4.3 Backbone comparisons 24
Table 4.4 Image processing comparisons 25
Table 4.5 Weigh decay comparisons 27

LIST OF ABBREVIATIONS

Adam	Adaptive Moment Estimation
AdamW	Adam Weight Decay
BreakHis	Breast Cancer Histopathological Database
BreCaHAD	Breast Cancer Histopathological Annotation and Diagnosis
CLAHE	Contrast Limited Adaptive Histogram Equalization
CNNs	Convolutional Neural Networks
DenseNet	Densely Connected Convolutional Networks
DL	Deep Learning
DNNs	Deep Neurol Networks
FN	False Negative
FP	False Positive
fpn	Feature Pyramid Network
H&E	Hematoxylin and Eosin
HSV	Hue Saturation Value
IoU	Intersection over Union
JSON	JavaScript Object Notation
mA F-score	Mean Average F-score
mAP	Mean Average Precision
mAS	Mean Average Sensitivity
MRI	Magnetic resonance imaging
R-CNN	Region-based Convolutional Neural Network
ResNet	Residual Network
RMSProp	Root Mean Square Propagation
RPN	Region Proposal Network
SGD	Stochastic Gradient Descent
SMDetector	Small Mitotic Detector
TP	True Positive
VGG	Visual Geometry Group
ViT	Vision Transformer

To my wife, Melek, and
my son, Mete

Chapter 1

Introduction

Breast cancer is the most prevalent cancer affecting women worldwide, accounting for 30% of all female cancers [1]. Annually, it is estimated that millions of cases are newly diagnosed, emphasizing the critical importance of early identification and subsequent intervention. The broad occurrence of this condition underscores the necessity to highlights the need to develop new methods of diagnosing and treating the disease [2].

Histopathological imaging, combined with mammography and MRI represent the crucial set of approaches for early detection of breast cancer. Mammography, which uses low-dose X-rays to find abnormalities in breast tissue, is widely recognized for its role in routine breast cancer screening. MRI, utilizing magnetic fields and radio waves, offers a complementary approach particularly useful in determining the magnitude of cancer and examining dense breast tissue. The approach involves the microscopic examination of tissue samples, enabling pathologists to pinpoint the presence of tumor cells with accuracy. Research indicates that histopathological analysis achieves higher degree of sensitivity in identifying early-stage cancers and differentiating between benign and malignant tumors than mammography and MRI, significantly affecting treatment the determination and outcomes [3], [4].

The integration of deep learning (DL) in medical imaging has induced a significant transformation, especially in the field of breast cancer detection. These sophisticated technologies reveal extraordinary precision when analyzing histopathological images, outperforming the analysis by humans. This is especially important due to the extensive amount of imaging data generated during breast cancer screenings, which presents a considerable challenge for manual analysis [5]. DL not only improves the diagnostic procedure but also minimizes the likelihood of human error, guaranteeing more reliable patient outcomes.

The differentiation between classification, segmentation, and detection within medical image analysis is fundamental. Classification categorizes images by the presence

of disease, segmentation accurately maps out tumor boundaries, and detection involves pinpointing the tumors' position in the images [6]. Precise tumor identification is critical in real-time applications, enabling precise tumor cell localization that leads to prompt and targeted treatment actions.

Numerous studies have focused on the classification of breast cancer in histopathological images, yet there's a significant gap in research focused on tumor cells detection, particularly regarding the Breast Cancer Histopathological Annotation and Diagnosis (BreCaHAD) dataset [7]. Numerous studies have utilized BreCaHAD dataset to improve classification efforts. In one study, Macedo et al. made us of deep learning techniques to classify the presence of tumor in histopathological images [8]. Likewise, Hlavcheva and colleagues investigated the application of Convolutional Neural Networks (CNNs) for distinguishing benign from malignant tumors, achieving improved classification performance [9]. Even with these progressions, challenges still persist, primarily because of the dataset's diversity in tumor morphology and staining practice, which can considerably alter the accuracy of classification. Deshmukh and their team also contribute to the field with their studies on classification [10]. Conversely, because object detection task is a more complex procedure compared to classification, leading to comparatively lower scores in terms of evaluation metrics. For example, Harrison et al. improved upon the performance of prior object detection models on the ICPR 2014 dataset, yet their results that were lower result than classification methods [11].

The efficacy of object detection models is greatly dependent on adjusting parameters such as the learning rate, weight decay, batch size, and feature pyramid, which can play a critical role in the model's capability to precisely identify key features in histopathological images [12]. Given the crucial significance of parameter optimization in augmenting the effectiveness of object detection models, this study aims to apply and determine the optimal parameters for tumor cell detection utilizing the BreCaHAD dataset. By conducting thorough experimentation and analysis, our goal is to overcome the shortcomings of current methods and contribute towards establishing more precise and trustworthy parameters for Faster R-CNN.

In conclusion, this research offers multiple contributions:

A thorough comparison has been conducted between fixed and adaptive box sizes for each cell within histopathological images, to establish the best box size for the BreCaHAD dataset. The study identifies the optimal box size that significantly improves the precision of tumor detection.

The investigation implements and assesses eight different image processing approaches to better the quality and efficacy of histopathological image analysis. Through careful assessment, we determine which techniques notably improve image sharpness and diagnostic accuracy, enhancing the effectiveness of tumor detection algorithms.

Through experimentation with different Fast R-CNN backbones, such as ResNet50, ResNet101, and MobileNetV3, we determine the optimal model architecture for processing the smaller datasets associated with histopathological images. This research helps in the selection efficient model architectures for medical image analysis, especially for datasets with limited in size.

Our research involved comparing four advanced optimization algorithms Adam, AdamW, RMSProp, and SGD, to find out which optimizer enhances our model detection in terms of F-score.

With the optimal model architecture established, we proceed to adjust hyperparameters like learning rate and weight decay to improve model performance further. Our organized method of hyperparameter optimization guarantees the model's effectiveness and accuracy in tumor cell detection within the BreCaHAD dataset.

Chapter 2

Literature Review

The integration of DL and image processing, particularly through the use of Convolutional Neural Networks (CNNs) such as Faster R-CNN, has substantially improved breast cancer detection and diagnosis processes. This part of the study synthesizes findings from new studies to explore the effectiveness, new developments, and particular results of different detection models and methods, aiming to increase the accuracy and efficiency of tumor cell detection.

Sophisticated image processing methods are vital for improving histopathological images' quality, thus improving the visibility and identification tumor cell. However, the restricted color variation within the BreCaHAD dataset has a minimal impact on F-score improvements, and some methods may even worsen the score. It is critical to note that images, have not done any processing process, showed a decline in F-score when certain image processing techniques were utilized [11]. Thus, the identification of suitable image processing techniques is essential. Their result in terms of F-score is given in the below Table the columns stand for L: Large size images, LN: Large size and color Normalized images, S: Small size images, and SN: Small size and color Normalized images.

Table 2.1 F-score comparisons of images by using normalization technique

Image	**L**	**LN**	**S**	**SN**
1-06	0.02	0.02	0.60	**0.61**
1-07	0.02	0	0.5	0.44
1-08	0	0	0.56	0.48
2-06	0.05	0	0.44	0.36
3-08	0	0.04	0.43	0.34
4-08	0	0	0.56	0.55
9-07	0.3	0.03	0.54	0.43
13-11	0	0	0.43	0.39

The significance of neural networks is well-established, leading to extensive research and discussions about them compared to other methods. A comparative analysis conducted by Daiel and team on different DNN architectures, including MobileNetV2, DenseNet201, EfficientNetB0, and Vision Transformer (ViT), highlights the distinct capabilities of these models in the domain of image classification [13]. Furthermore, Zhou et al. have embarked on a benchmarking study to distinguish classical techniques from deep neural networks [14]. Concurrently, Jawad et al. executed detailed examination of DenseNet, with a specific focus on DenseNet121, for the purpose of classification [15].

Due to the limited number of samples in specific datasets like BreCaHAD, frequently requires the integration of datasets, like the Breast Cancer Histopathological Database (BreakHis), with the aim of enlarging sample sizes and training more effective models [16]. Architectures including VGG16, VGG19, ResNet50, and ResNet101 have been applied to achieve this goal [17]. CNN model success in medical imaging is evidenced by their application to the TUPAC16 dataset [18]. The research by Ilyas, concentrates on detection tumor cells by using a ResNet50 architecture has yielded higher accuracies in this domain [19]. Moreover, the use of CNNs, including Faster R-CNN and the SMDetector, has played a key role in identifying breast cancer. With its modified ResNet101 backbone, the SMDetector has achieved good performance, exceeding the capabilities of existing models in aspects of precision, recall, and F-score [20]. Below table show the results of proposed models in terms of F-score in ICPR 2014 dataset.

Table 2.2 Comparison object detection models

Detection Model	**Precision**	**Recall**	**F-score**
DeepMitosis	43.10	44.30	43.70
SmallMitosis	51.20	47.90	49.50
PartMitosis	66.40	50.70	57.50
SMDetector	68.49	59.86	**63.88**

Optimizers play an important role for the overall performance of deep learning models. The optimizers Adam, AdamW, and SGD are among the commonly used optimizers for their unique strategies in adjusting learning rates and applying other hyper parameters. Recent research has evaluated the effectiveness of Adam, AdamW, and SGD across a range of deep learning models and tasks. For instance, a detailed analysis by Wilson et al. has pointed out the pros and cons of adaptive optimizers like Adam and

RMSprop versus to SGD, indicating that adaptive techniques may not always guarantee improved generalization [21]. Additionally, a study conducted by Chen et al. has investigated the performance of Adam and SGD in training deep neural networks, showing that although Adam facilitates quicker initial convergence, SGD may offer better long-term performance [22].

Hyperparameter optimization consists of adjusting parameters including learning rate, weight decay, and various other factors to optimize a model's effectiveness. The study performed by Smith et al. on the implementation cyclic learning rates demonstrates the considerable advantages of employing dynamic learning rate strategies, which in dramatically reducing training times and improving the result in terms of F-score [23]. Furthermore, the implementation of Bayesian optimization strategies for optimizing hyperparameter in deep learning frameworks has shown good results, especially in sophisticated models used for histopathological image analysis [24]. In addition, Esteva et al.'s study showing the importance of hyperparameter optimization in accomplishing dermatologist-level accuracy in the classification of skin cancer by using CNNs [25].

Chapter 3

Materials and Methods

Through this study, we investigating five crucial factors in order to accurately detect tumor cells by using the BreCaHAD dataset. Our primary focus is to determine the most efficient methods for analyzing histopathological images. The main goal of this research, not only seek to identify the most optimal techniques for these types of applications but also aims to find any potential shortcomings or redundancies that may occur when utilizing certain approaches in this specific tasks. By performing iterative testing using diverse configurations enable us to identify the optimal setup. Then, we methodically adjusted one parameter to evaluate its effect on the model's performance metrics in terms of precision, recall and F-score. Our assessment covers a wide range of factors like box size, batch size, image processing approaches, optimization techniques, the architecture employed in the Faster R-CNN model, and hyperparameter optimization. The entire structure of our method is outlined in Figure 3.1.

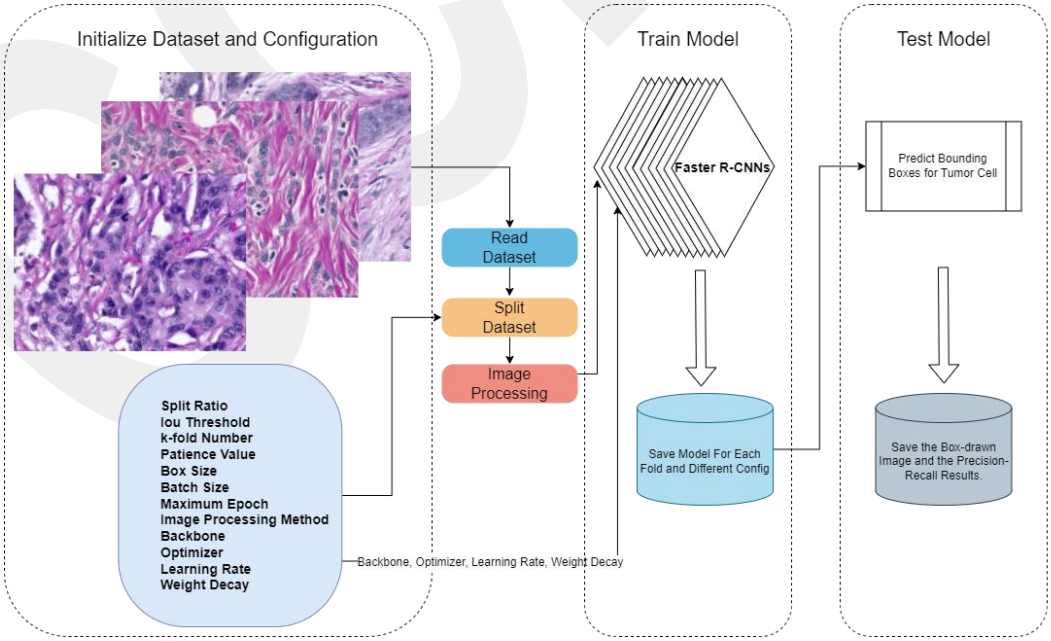

Figure 3.1 General structure of our proposed method

3.1 Dataset

The BreCaHAD dataset serves as the foundation for this research, offering publicly accessible archive created to contribute studies in automated tumor cell detection in breast cancer detection by using histopathological annotated image analysis. This dataset contains 162 whole slide images of breast tissue, all annotated by professional pathologists for detailed study [7].

In image-based studies, resolution is crucial factor. In BreCaHad dataset, every image is captured at a resolution of 1360 x 1024 pixels. These images, stained with H&E to identify six different cell types. Each image in the dataset comes with annotations in JavaScript Object Notation (JSON) format, detailing the class types of cells and their locations within each image. As indicated in Table 3.1, a significant portion of the dataset is comprised of tumor nuclei cells.

Table 3.1 Distribution of cell types by annotation colors

Cell Type	**Color**	**# of Annotations**
Mitosis	Orange	115
Apoptosis	Green	271
Tumor Nuclei	Blue	20,155
Non-tumor Nuclei	Pink	1,905
Tubule	Light Blue	493
Non-tubule	Yellow	610
Total		**23,549**

The BreCaHAD dataset is an important resource for examining tumor detection in breast cancer tissues through histopathological images, but there are some obstacles due to the small number of instance and the unbalanced cell types. Amont the 23,549 cells featured the dataset, 20,155 are classified as tumor cells, with only 3,394 samples categorized into five other classes. This significant imbalance highlights that most of the data is focused on tumor cells, complicating the detection of other cell types within the entire image. Ground truth images assign a unique color to each cell type, as shown in Figure 3.2.

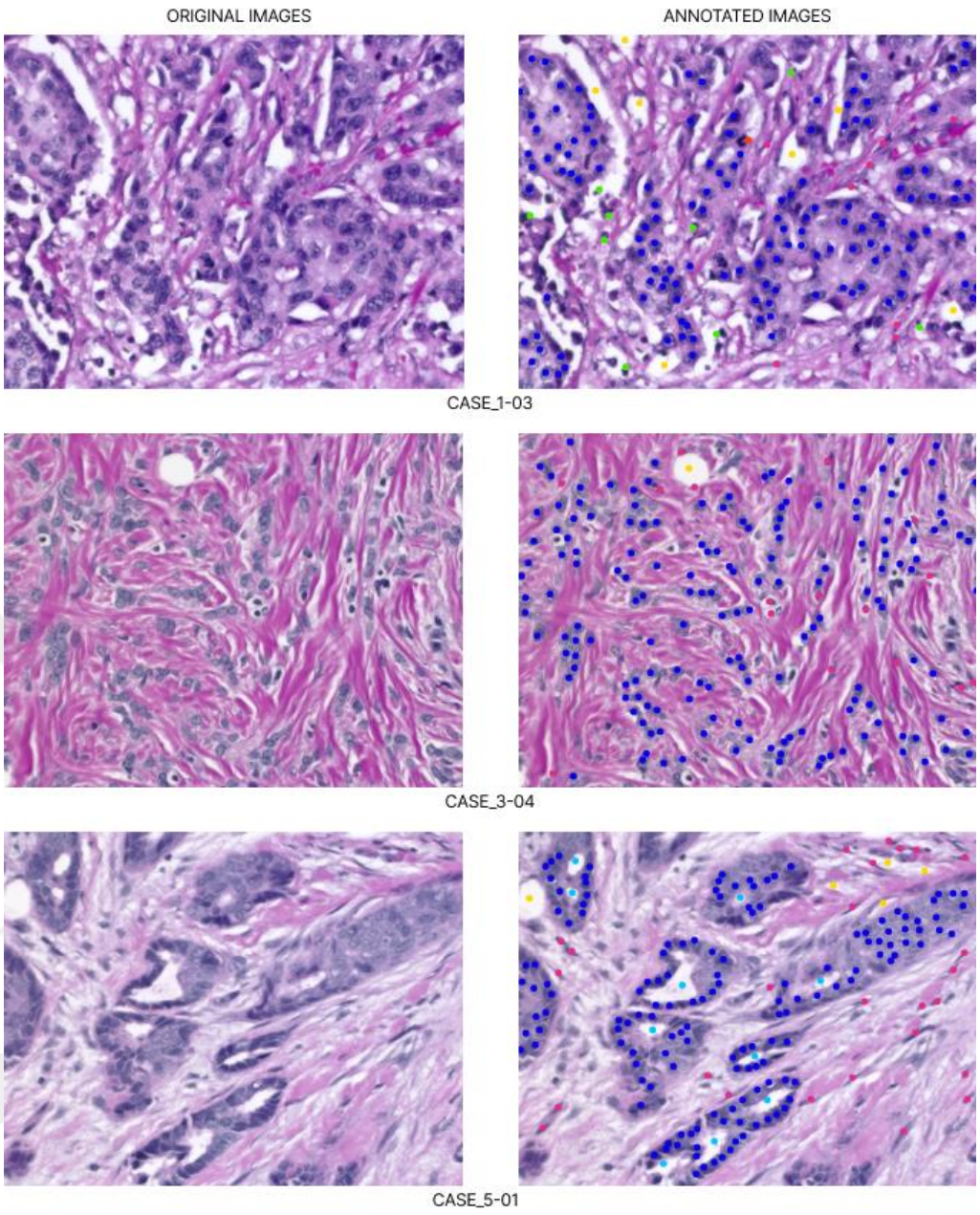

Figure 3.2 Original images and annotated images

3.2 Algorithm

Our algorithm is configured to be adoptable, focusing on comprehensively testing different parameter setups to decide the best configuration setup for object detection task.

Algorithm 1: Tumor Cell Detection Algorithm by Using Faster R-CNN

Establish a Connection with Google Drive:
    Connect to Google Drive
    Retrieve dataset
Load Configuration Settings:
    Load 'configurations.json'
    Extract initial setup and run-specific parameters
Image Processing: *Process images according to the specified configuration.*
Partition the Dataset:
    Split dataset into training and testing subsets by using defined ratio for partitioning in config file
Designate Computing Device:
    Set device = "cuda" to leverage GPU acceleration
Execute Training Procedure:
    Get 'k' value from config file for k-Fold Cross Validation
for *each fold* ***do***
    Model Initialization:
        Select pre-trained architecture and optimizer
    Shuffle and Partition Dataset:
        Shuffle the dataset randomly
        Partition for k-fold methodology
        Implement on datasets
    Load Datasets:
        Extract labels and calculate exact box locations
    Define Early Stopping Criterion:
        Set patience value
    Training Epochs:
    Model Training:
        Utilize zero-gradient loss function
    Epoch Termination:
        Terminate if hit early stopping condition or reach max epoch number
    Store Model

31: ***end for***

32: ***Testing Procedure:***

33: *Retrieve Trained Model*

34: *Predict Bounding Boxes*

35: *Evaluate Metrics*

36: *Save results*

3.3 Image Processing

Identifying tumor cells in histopathological images, particularly those stained with Hematoxylin and Eosin (H&E), presents considerable obstacles. Image processing techniques are implemented to increase the diversity and size of training dataset. However, due to the distinct nature of histopathological images, not all techniques prove to be effective.

In our research, we analyzed eight unique image preprocessing techniques to determine their effects on the F-score. These techniques are color normalization by using Contrast Limited Adaptive Histogram Equalization (CLAHE), denoising, sharpening, brightness adjustment, Gaussian pyramid, HSV color normalization, and finally Sobel filtering.

- **Color Normalization (CLAHE):** Applying CLAHE for color normalization makes pictures clearer by boosting contrast, beneficial for examining tissue images in detail without adding noise [26].
- **Denoising:** Noise reduction in images ensures the preservation of significant details while getting rid of irrelevant pixels. The Non-Local Means techniques is particularly effective for this, as it analyzes the whole image to preserve clear edges, which is crucial for accurate examination of tissue images [27].
- **Sharpening:** Sharpening images emphasizes textures and edges, essential for detecting and separation of tumor cells in histopathological images [28].
- **Brightness Adjustment:** Altering an image's brightness can improve the detection details in images which is essential for diagnosing [29].
- **Gaussian Pyramid:** The Gaussian Pyramid method allows for the examination of images at various scales, which is helpful for detailed exploration of histopathological images [30].

- **Color Normalization (HSV):** Modifying colors in the HSV spectrum corrects for differences in lighting and staining in these images, aiding models to identify patterns and anomalies [31].
- **Sobel Filtering:** By calculating the intensity gradient of the image, Sobel Filtering identifies edges, that helps emphasizing significant components in tissue images [29].

3.4 Faster R-CNN

The progression from R-CNN to Faster R-CNN marks significant milestones in object detection, each version improving on the last in terms of speed, accuracy and functionality. This section examines these technological advances, the critical role CNNs play in object detection, and the specific advantages presented by Faster R-CNN. Further, we introduce the concept of backbones, concentrating on particular architectures like ResNet50 and MobileNetV3, and their importance in improving object detection.

Region-based Convolutional Neural Networks (R-CNNs) employ CNNs to identify and classify specific image areas as object proposals. This approach extends the capabilities of standard CNNs by adding a targeted object detection mechanism, which significantly refines the model's ability to extract features. Although R-CNNs have marked a significant advancement in object detection, their computational efficiency is compromised by the need to process numerous region proposals independently. This limitation significantly challenges their practical application, necessitating further innovations in object detection techniques to enhance speed and efficiency [32].

Fast R-CNN enhanced R-CNN’s approach by implementing shared computation across the entire image, markedly increasing efficiency and performance. Nonetheless, Fast R-CNN continued to depend on external mechanism for proposal generation still served as a bottleneck [33].

Faster R-CNN eliminated the bottleneck in proposal generation by integrating the Region Proposal Network (RPN) directly into the network, allowing for the generation of proposals to be part of the network's workflow. This advancement enabled real-time performance without sacrificing accuracy [34]. The model was utilized with a pre-trained version on the Common Objects in Context (COCO) dataset [35]. The entire process of transfer learning involved initializing the network with pre-trained weights and systematically fine-tuning the parameters to better suit our breast cancer histopathological

images. Throughout this process, various hyperparameters, such as learning rates, batch sizes, and epochs, were meticulously adjusted.

The integrated architecture of Faster R-CNN facilitates end-to-end training, significantly diminishing processing durations and establishing it as an optimal method for real-time object detection tasks. The use of advanced backbone architectures also enhances its capability to extract complex features effectively [34]. The Faster R-CNN architecture is given in Figure 3.3.

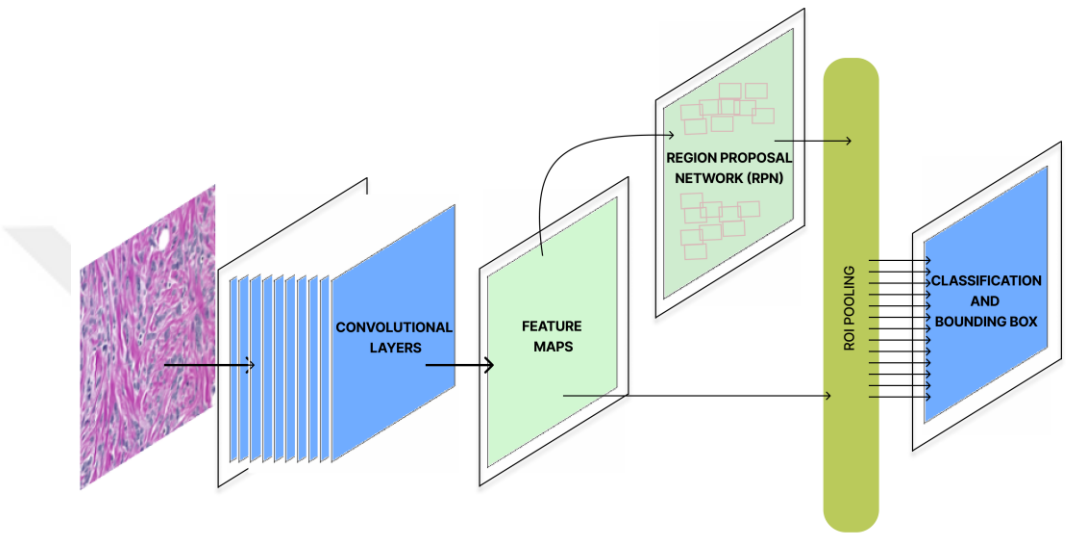

Figure 3.3 Faster R-CNN architecture

The backbone of an object detection network is the set of CNNs designated for feature extraction tasks. By using pretrained weights, commonly sourced from models trained on comprehensive datasets like ImageNet, serve as a good starting point for training, facilitating quicker convergence and elevated detection efficiency, especially when training dataset is limited [36]. ResNet, characterized by its residual connections, enables training of much deeper neural networks. The versions ResNet50 and ResNet101 correspond to ResNet configurations with 50 and 101 layers, accordingly [37]. MobileNetV3 is designed for mobile and limited resource environments. It achieves a balance between performance and accuracy. MobileNetV3 (fpn) models differ in terms of scale and capacity, making them adaptable to different computational constraints [38].

3.5 Optimizer

Choosing the most suitable optimizer technique is crucial for improving the result precision and sensitivity. Assessing the efficiency of ddifferent optimization algorithms, such as SGD, Adam, AdamW, and RMSProp, is examined in relation to these pre-trained models.

- **SGD**: Stochastic Gradient Descent (SGD) adjust parameters based on the gradient of the loss function concerning the parameter. Due to its simplicity and efficiency in a variety of machine learning applications, SGD is often used as a benchmark optimizer in a academic and practical of studies [39].
- **Adam**: Adam, or Adaptive Moment Estimation, calculates adaptive learning rates for individual parameters by integrating the benefits of AdaGrad and RMSProp. Adam is preferred for its rapid convergence and efficiency with sparse gradients [40].
- **AdamW**: ADAMW presents a new approach by deploying a decoupled weight decay regularization strategy, addressing the shortcomings of Adam's L2 regularization. This advanced technique ensures that weight decay is independent of gradient updates, thus optimizing the overall performance of the optimization process [41].
- **RMSProp:** RMSProp modifies the learning rate for each parameter by dividing the learning rate by a moving average of the gradients' magnitudes, addressing the challenge of reducing learning rates seen in AdaGrad. This technique is highly effective in online and non-stationary conditions [42].

For optimizer methods, learning rate and weight decay are very important. The learning rate plays pivotal role in deciding the step size at each iteration to minimizing the loss function. Selecting the right learning rate is critical for ensuring the model quickly converges to the minimum loss, preventing the model from overshooting or getting stuck in local minima. Meanwhile, weight decay is utilized for regularization, penalizing large weights to prevent overfitting. Optimizing these hyperparameters is vital for enhancing the model's performance, maintaining its stability, and improving generalization capability [43].

3.6 Parameter Optimization

In object detection models, especially within medical imaging where the accurate identification of cellular formations is critical, the optimization of bounding box sizes plays a key role. Our analysis covers the application of both adaptive and fixed bounding box sizes. While fixed bounding boxes provide constant size, which simplifies the model training process, adaptive bounding boxes from the "BreCa_v5 Dataset" annotations that are changing size of box according to each cell morphological structure [44].

Modifying batch sizes during training process is crucial for determining best precision and recall, and also it is crucial for evaluating the model's effectiveness. The selection of batch size affects the learning dynamics within deep learning models. It involves balancing computational resources with accuracy of the model. Optimal batch size selection increasing the learning process, making it as a crucial factor in maximizing the performance of deep learning implementations [45].

Chapter 4

Experimental Results

The finding of our comprehensive experimental analysis is presented in this section, focusing on the effects of different model configurations and optimization strategies on the performance of algorithm. The outcomes of our study provide important perspectives on optimizing deep learning models for histopathological image analysis to detect tumor cell, key considerations for improving accuracy and efficiency.

The configuration parameters were meticulously chosen in order to optimize the algorithm's performance while maintaining standards for speed and efficiency:

- **IoU Threshold:** Set at 0.5, this parameter is a key to assess the precision of bounding box predictions in comparison to ground truth images.
- **Splitting Ratio:** A partition of 90% for training and 10% for testing was implemented to guarantee a thorough training dataset while preserving a representative test set for evaluation.
- **Patience Value:** To prevent overfitting, we implemented an early stopping mechanism. In this algorithm to stop epoch there is a patience value which is set 7. So that, we guarantee a balance between sufficient model training and the prevention of overtraining on the dataset.
- **Maximum Epochs:** If early stopping mechanism is not triggered, we set the maximum epoch number is 100.
- **Tested Parameters:** Initially, we ran all combinations of box size, batch size, optimizing algorithm, and learning rate on the original image and determined the best four parameters. Then, these parameters were held constant, and the model was retrained on the original image for three other backbones, finding the best backbone. With these four parameters and the backbone fixed, the model was run for seven different image processing techniques, and the best image processing technique was identified. Finally,

keeping the best image processing technique constant, the effects of three different weight decays were analyzed by altering them.

4.1 Environmental Setup

Our study's algorithms were implemented with Python version 3.7, known for its abundant libraries and strong support within the scientific computing and machine learning communities. For our experiments, we used the advanced functionalities offered such as torch.vision by PyTorch. Execution was facilitated on Google Colab (colab.research.google.com). The environment we utilized featured a Tesla V100 GPU, augmented by a high memory capacity of around 51 GB RAM, 16 GB dedicated to GPU memory, and 200 GB of available disk space that is enough for our demanding computational needs. Additionally, our dataset was hosted on Google Drive, offering direct and easy access from withing the Colab environment.

4.2 Performance Evaluation Metrics

To evaluate the performance of our implemented algorithm in breast cancer detection using Faster R-CNN, we depend on key metrics such as IoU, Precision, Recall, and F-score. These metrics help us a comprehensive understanding of the model's accuracy and its success in spotting and categorizing tumor cells in histopathological images.

4.2.1 Intersection over Union (IoU)

IoU is the most popular metric in object detection tasks that measures the overlap between the predicted and the actual bounding boxes [46].

$$IoU = Area\ of\ Overlap\ /\ Area\ of\ Union \tag{4.1}$$

higher IoU score means the object detection model is more accurate. In our research, we set an IoU threshold to classify detections as either true positives or false positives.

4.2.2 Precision and Recall

Precision and Recall are essential for assessing the performance of trained model, especially in the context of histopathological imaging where both false positives and false negatives have significant consequences.

Precision (Positive Predictive Value) measures the proportion of correctly identified positive cases out of all cases that were identified as positive.

$$Precision = TP / (TP + FP) \quad (4.2)$$

Recall (Sensitivity) measures the proportion of actual positives that were correctly identified.

$$Recall = TP / (TP + FN) \quad (4.3)$$

where TP represents true positives, FP represents false positives, and FN represents false negatives [47].

4.2.3 F-score

The F-score is a metric that combines Precision and Recall by calculating their harmonic mean. It is valuable for achieving a balance between Precision and Recall.

$$F - score = 2 \times (Precision \cdot Recall) / (Precision + Recall) \quad (4.4)$$

Taking into consideration the precision and recall of all relevant instances, the F-score provides a singular metric to analyze the overall performance of the model [48].

4.3 Proposed Method

Our findings are visually presented in Figure 4.1, Image (a) is the original histopathological breast cancer image, and image (b) showcases the tumor detection accomplished by our model. The ground truth boxes are denoted by blue in image (b), and the detected tumors are represented by green boxes. Image (c) specifically highlights the accurate detections (IoU >= 0.5), demonstrating the precision of our model. Image (d) specifically highlights the missed detections, indicating areas for improvement. Images (e) and (f) illustrate false positives, with image (e) displaying incorrect detections and image (f) exhibiting cases with an IoU value below 0.5. These images emphasize the challenge of distinguishing similar cellular structures.

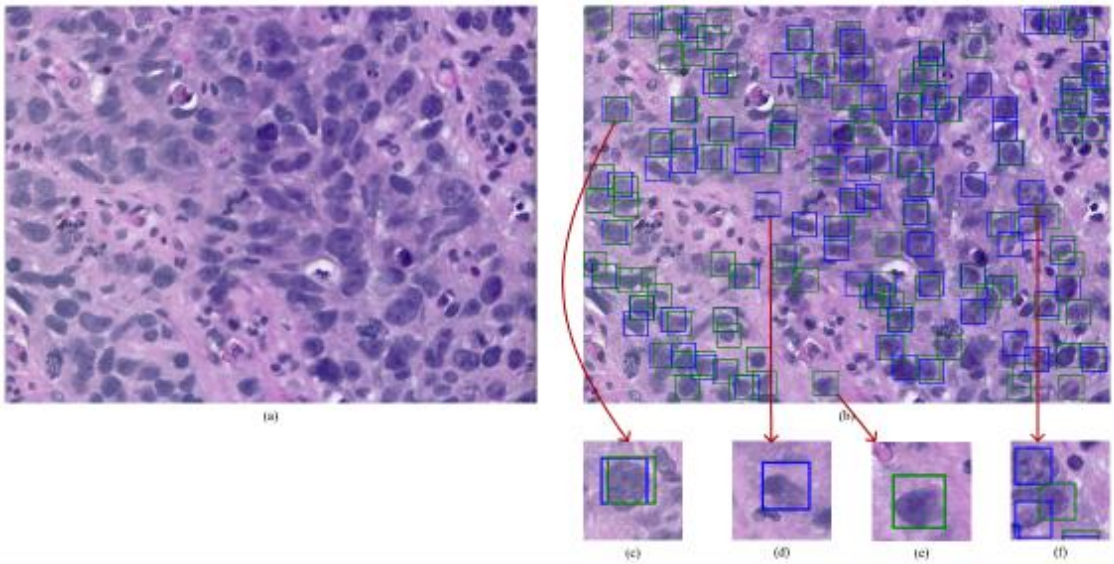

Figure 4.1 Original image vs predicted boxes image

The algorithm was optimized by analyzing the values tested in Table 4.1.

Table 4.1 Parameters and tested values

Parameters	**Values**
Box Size	32, 64, Adaptive
Batch Size	4, 8
Image Processing	brightness adjustment,color normalization (CLAHE),denoising, gauss pyramid, gauss pyramid with sharpening, color normalization (HSV), sharpening, sharpening with denoising, sharpening with gauss pyramid, sobel filtering
Backbone	MobileNetV3, ResNet101, ResNet50,ResNet50 (fpn v2)
Optimizer	Adam, AdamW, RMSProp, SGD
Learning Rate	0.001, 0.003, 0.01, 0.03, 0.1
Weight Decay	0.01, 0.05, 0.1

4.3.1 Configuration Parameters of Proposed Method

A key element of our implementation is a configuration file, carefully designed to distinguish between constant and variable parameters during the training process. This file is divided into two sections:

- **Constant Parameters:** During the different training cycle, some values are kept constant to serve as a stable basis for evaluating the performance of the algorithms.
- **Variable Parameters:** The dynamic configurations consist of parameters such as box size, batch size, learning rate, weight decay, the method of optimization, and image processing strategies, support a detailed investigation into the various parameter spaces.

4.3.2 Data Splitting

After deciding our configuration framework, we split the dataset into training and testing segments based on a pre-determined ratio, ensuring evaluation consistency. To enhance the model trustworthiness, we integrated k-fold cross-validation and an early stopping algorithm. These enhancements not only amplify the model's ability to generalize but also prevent against overfitting.

4.3.3 Image Processing

Image processing techniques selected beforehand were implemented on both the training and testing datasets. The process of training involved iterative adjustments to determine the optimal epoch value at which peak performance was observed. This model then saved on Google Drive for future use and examination.

4.3.4 Model Training

Our implementation fundamentally involved exploring different backbone architectures, as the feature extractor component in the Faster R-CNN framework. We particularly focused on the effects of employing ResNet50 and ResNet101, known for their powerful residual learning capacities and their ability to significantly improve tumor cell detection by offering rich feature representations.

An important component of our training strategy was the exploration of various optimizer methods. The goal was to discover the optimizer that best effective one with the Faster R-CNN model and specific backbone architectures utilized. We looked at optimizers like SGD, Adam, AdamW, and RMSProp. Each one has its own distinct advantages, such as faster learning speeds and better handling of sparse gradients. Then,

we adjusted key settings like the learning rate and weight decay to improve our model's accuracy and efficiency. We carefully adjusted the learning rate to find a balance between how fast the model trained and the achieving the lowest loss value. Likewise, we used weight decay to keep model from overfitting, ensuring the model can generalize to test and validation dataset [49].

4.3.5 Test Model

After reaching the best training, we shifted to testing procedure. The trained model was applied to previously unseen images in the test set. This phase was crucial for testing how well our model works in real-life. We focused on how accurate and efficient. We concentrated on evaluating its precision, recall, and F-score, which were influenced by the Intersection over Union (IoU) threshold.

To provide a detailed assessment of the model's effectiveness, we check three important benchmarks: mean Average Precision (mAP), mean Average Sensitivity (mAS), and mean Average F-score (mA F-score). Here, "mean" refers to the arithmetic mean calculated from the results of various cross-validation folds, ensuring the consistency and reliability of our findings.

- **mAP:** This measure evaluates the precision of the model's bounding box predictions against the ground truth data, considering k-fold cross validation. A best mAP value indicates more precise localization of detected areas within images.
- **mAS:** Indicating the model's average sensitivity or recall across multiple folds, the metric show that the model’s effectiveness in accurately identifying all true positive instances. Higher mAS scores shows that a better capability in determining tumor cell.
- **mA F-score:** Acting as the harmonic mean of precision and sensitivity, the F-score provides a comprehensive assessment of the model's performance. The mean Average F-score aggregates this balance over different folds.

4.4 Optimizing Parameters

We ran all combinations of four basic parameters: box size, batch size, optimizer, and learning rate. For these four different parameters, a total of 120 different combinations were executed, each with 5 folds, totaling 600 model trainings, takes around

fifteen days. The best 20 results are provided in the table below. As can be seen from this table, the best results were achieved with a box size of 64, a batch size of 4, an optimizer of AdamW, and a learning rate of 0.001.

Table 4.2 Results of combinations: Box Size, optimizer, batch size, learning rate

Box Size	**Optimizer**	**Batch Size**	**Learning Rate**	**mAP**	**mAS**	**mA F-score**
64	**AdamW**	**4**	**0.001**	0.7812	0.5894	**0.6718**
64	SGD	4	0.001	0.7878	0.5817	0.6691
64	AdamW	8	0.001	0.7798	0.5833	0.6672
Adaptive	AdamW	4	0.001	0.7268	0.5969	0.6554
64	AdamW	4	0.003	0.7662	0.5692	0.6527
64	SGD	8	0.003	0.7796	0.5597	0.6516
Adaptive	AdamW	8	0.001	0.7234	0.5899	0.6497
64	AdamW	8	0.003	0.7512	0.5701	0.6482
64	SGD	8	0.01	0.7932	0.5461	0.6462
Adaptive	SGD	8	0.01	0.7205	0.5850	0.6456
Adaptive	SGD	4	0.01	0.7267	0.5802	0.6451
Adaptive	SGD	4	0.003	0.7190	0.5809	0.6426
64	SGD	8	0.001	0.7774	0.5437	0.6398
Adaptive	SGD	8	0.003	0.7116	0.5785	0.6381
Adaptive	AdamW	4	0.003	0.7074	0.5784	0.6363
Adaptive	SGD	4	0.001	0.7080	0.5774	0.6360
64	AdamW	8	0.01	0.7656	0.5443	0.6355
Adaptive	SGD	4	0.03	0.7118	0.5685	0.6320
Adaptive	SGD	8	0.001	0.7052	0.5698	0.6303
64	SGD	8	0.03	0.7721	0.5294	0.6270

Testing different sizes of bounding boxes revealed significant insights into their effect on model accuracy. Fixed-dimension bounding boxes demonstrated better performance than those with variable box size of cell. This observation emphasizes the significance of uniform object detection, particularly in the context of tumor cell detection, where mA F-score is key metric.

The study explored fixed bounding box sizes of 32x32, and 64x64 pixels, alongside a contrasting approach using a separate annotation file that prescribed a unique bounding box size for each cell. The outcomes presented in Table 4.2 detail the performance differentials across adaptive bounding box sizes utilized within our model, including an evaluation of adaptive box sizes.

Table 4.2 reveals that the bounding box size of 64 delivers the most optimal and balanced results, as evidenced by the highest mA F-score.

The results propose an ideal batch size that balances computational efficiency with the skill to effectively generalize across the training data. Table 4.2's results provide an in-depth view of the effects various batch sizes have on the model's detection capabilities. It finds that a batch size of 4 yields the best performance, achieving a peak mean Average F-score of 0.6718. As a result, this discovery highlights the pivotal role batch size plays in deep learning models for complex detection tasks.

Optimizers play an important role for achieving best model performance. Detailed analysis of SGD, Adam, AdamW, and RMSProp optimizers, we explore on their distinct impacts on the training behaviors and final scores by the model.

The detailed comparison in Table 4.2 highlights the effects of various optimizers on our model's detection capabilities. Among the optimizers tested, AdamW distinguishes itself as the best optimizer.

The performance of Adam and SGD is closely matched in terms mAP and mAS demonstrating their potential applicability in similar jobs. Nonetheless, the significantly lower performance of RMSProp, especially in its mA F-score, indicates its limited scope in this specific context.

The learning rate stands as a crucial impacts the training process's velocity and quality. Through methodical testing, we pinpointed the ideal learning rate configuration that ensure rapid convergence alongside the model’s ability to recognize complex patterns in the dataset.

Table 4.2 offers a comprehensive examination of the effects of different learning rate setups on the tumor cell detection capabilities of our algorithm. The finding reveals a distinct optimization stand outs with a learning rate of 0.001, showcasing the highest values in every performance measure.

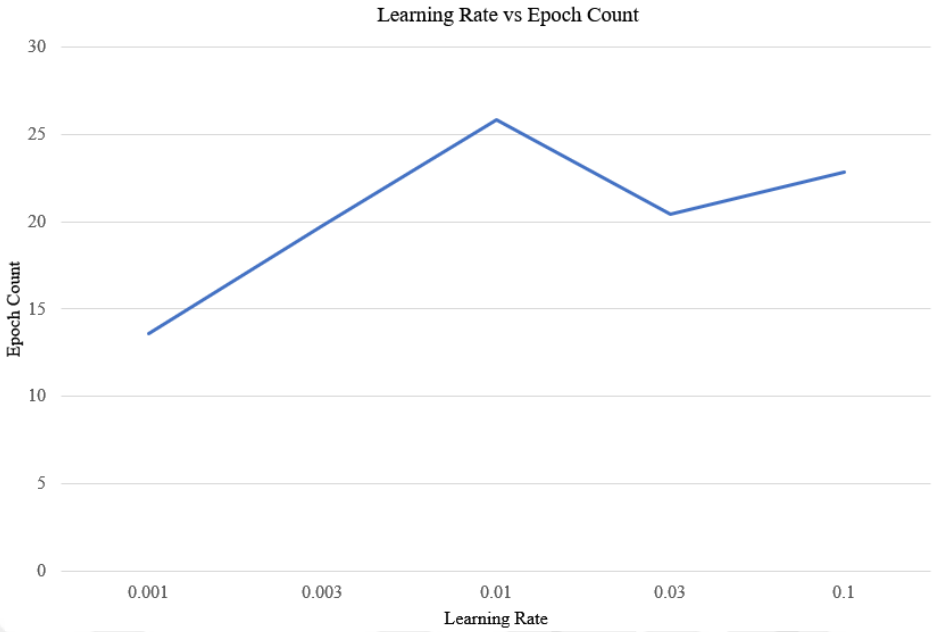

Figure 4.2 Epoch vs learning rate

Figure 4.2 offers a visual demonstration between learning rates and the total number of epochs required for model training. The graphic demonstrates how the model's convergence speed varies with different learning rate settings. A reduced learning rate, such as 0.001, leads to the model necessitating fewer epochs. Conversely, an increase in the learning rate results in an elevated need for epochs, peaking at a learning rate of 0.01 with 25 epochs required. Remarkably, when the learning rate assign to 0.03, there's a slight reduction in epoch numbers.

4.5 Backbone Benchmarks

The decision on backbone architecture is important the feature extraction efficiency of the Faster R-CNN model. Through our analysis of ResNet50, ResNet101, and MobileNetV3 architectures sheds light on how each impacts the model's detection capabilities and accuracy comprehensively.

Table 4.3 Backbone comparisons

Backbone	**mAP**	**mAS**	**mA F-score**
MobileNetV3	0.6617	0.4144	0.5096
ResNet101	0.7646	0.5632	0.6486
ResNet50 (fpn)	0.7630	0.5582	0.6447
ResNet50 (fpn v2)	0.7812	0.5894	**0.6718**

Summarized in Table 4.3, the comparative study showcases the performance of various Faster R-CNN backbones in our breast cancer detection model. Among the evaluated backbones, ResNet50 (fpn v2) proved to be the most efficient, achieving the top mA F-score of 0.6718.

Additionally, the findings reveal a significant performance variation across the backbones. Among the legacy ResNet architectures like ResNet101 and the ResNet50 (fpn) delivering potent results, but ResNet50 (fpn v2) is achieved the best score. In contrast, models based on MobileNetV3 backbones showed lower performance metrics.

4.6 Finding the Optimal Image Processing

Preparing images through preprocessing is essential for accurate and efficient data analysis. The findings in Table 4.4 outline a thorough analysis of the distinct effects that different preprocessing methods over the performance of our tumor detection model. Out of the various preprocessing techniques applied, the best one is sharpening technique stood out, achieving the best mA F-score of 0.6737.

Table 4.4 Image processing comparisons

Image Processing Technique	**mAP**	**mAS**	**mA F-score**
Original	0.7812	0.5894	0.6718
Brightness Adjustment	0.7812	0.5874	0.6706
Color Normalization (CLAHE)	0.7699	0.5856	0.6652
Denoising	0.7742	0.5829	0.6651
Gauss Pyramid	0.7822	0.5857	0.6698
Gauss Pyramid with Sharpening	0.7850	0.5867	0.6715
Color Normalization (HSV)	0.7621	0.5816	0.6597
Sharpening	0.7938	0.5851	**0.6737**
Sharpening with Denoising	0.7777	0.5854	0.6680
Sharpening with Gauss Pyramid	0.7825	0.5820	0.6675
Sobel Filtering	0.7545	0.5587	0.6420

Figure 4.3 showcases the advancements histopathological images following the implementation of image processing techniques. Especially, merging the Gauss Pyramid with Sharpening has led to good improvements, highlighting that the combination of

various preprocessing techniques can improve the performance of the model. However, despite its benefits in edge detection, Sobel Filtering was found to be less efficient in this context, as indicated by its reduced mean Average F-score.

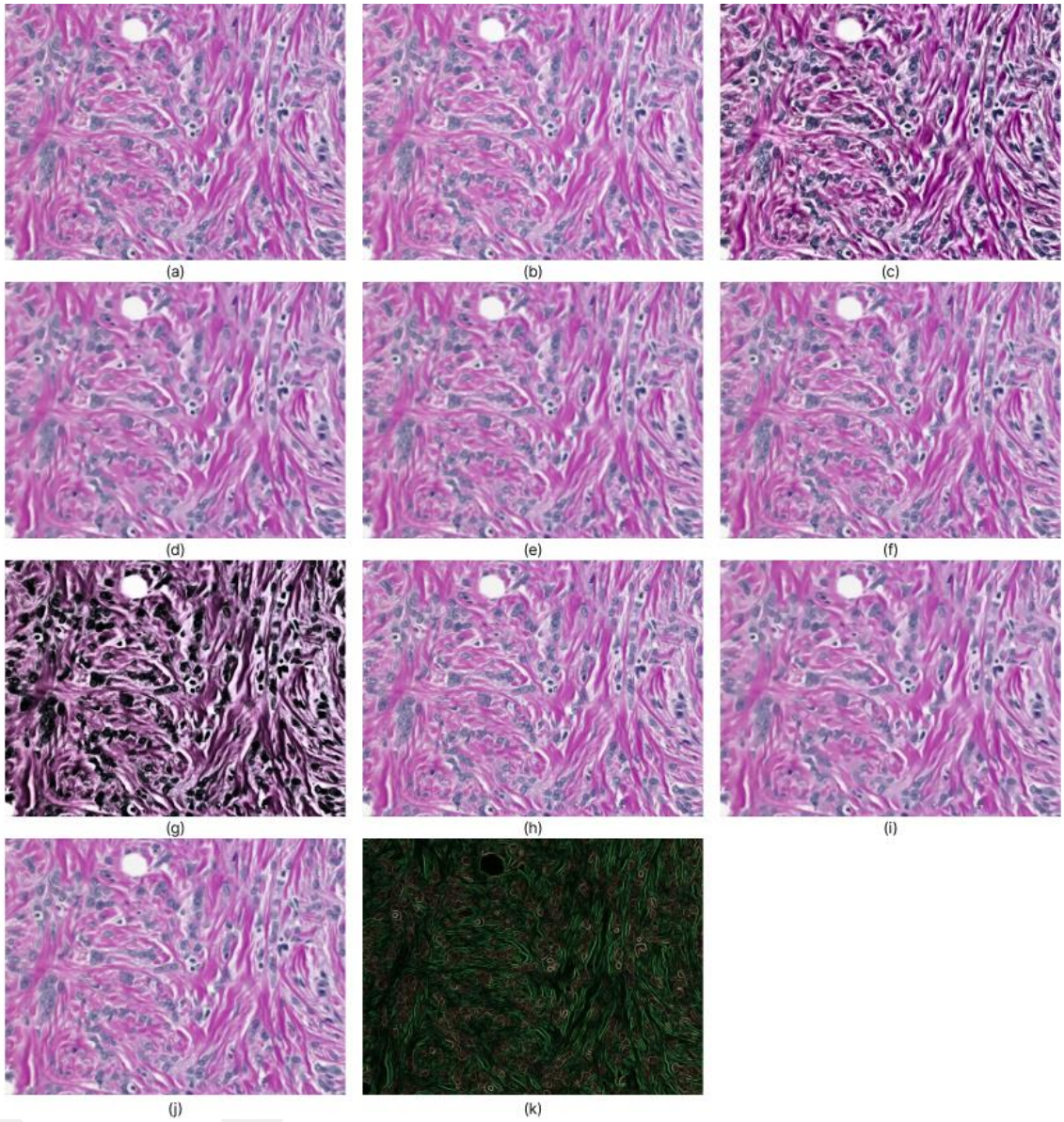

Figure 4.3 Applied image processing techniques

According to Figure 4.3, the applied image preprocessing techniques are represented in the following order: (a) original image, (b) brightness adjustment, (c) color normalization (CLAHE), (d) denoising, (e) Gaussian pyramid, (f) Gaussian pyramid with sharpening, (g) color normalization (HSV), (h) sharpening, (i) sharpening with denoising, (j) sharpening with Gaussian pyramid, and (k) Sobel filtering.

4.7 Weight Decay Optimization

Finally, we explored the role of weight decay in model regularization and its preventive role against overfitting. By fine-tuning the weight decay parameter, we found a balance that enhances the model's generalization capabilities, improving performance on test data.

Table 4.5 Weigh decay comparisons

Weight Decay (WD)	mAP	mAS	mA F-score
0.01	0.7938	0.5851	**0.6737**
0.05	0.7878	0.5784	0.6671
0.1	0.7894	0.5856	0.6724

The data presented in Table 4.5 shows that the influence of different weight decay parameters on the efficacy of our detection model. The configuration with a weight decay of 0.01 stands out for delivering the top mean Average F-score of 0.6737, signifying the optimal balance between model accuracy and its ability to detect relevant instances.

While a weight decay of 0.1 leads to a minor improvement in mAS. That is potential in improving the model’s sensitivity, the overall best performance in terms of mA F-score is attained with the lowest weight decay value assessed. This finding demonstrating the effect that weight decay has on model training, implying that a reduced weight decay offers better results.

Chapter 5

Conclusions and Future Prospects

5.1 Conclusions

This research has conducted on a detailed examination at enhancing the identification of tumor cells within breast cancer histopathological images, by adapting an integrated method that combines deep learning along with image processing techniques.

The findings of this study are significant, and diverse. The analysis of the most effective bounding box sizes demonstrated that fixed-size boxes, especially those measuring 64 pixels. This is show that traditional favoring of variable-size annotations is not a state-of-art. The result highlights the critical importance of uniform feature representation, an essential component for the effectiveness of deep learning models in analyzing histopathological images.

Additionally, a detailed comparison of various image preprocessing methods revelated that sharpening technique as the most useful method to improve model performance. This finding highlights the crucial impact of preprocessing on the preparation of histopathological images for analysis, boosting the model's ability to precisely detect tumor cells.

Our analysis of various backbone architectures for Faster R-CNN has improved our understanding of feature extraction in deep learning models. The exceptional performance of the ResNet50 (fpn v2) architecture underscores the critical need for selecting an appropriate backbone that meets the model's objectives, and diagnostic sensitivity. Additionally, our evaluation of different optimizers has revealed AdamW as the most effective, particularly distinguished by contribution to achieving the highest mA F-score.

As a conclusion, the careful adjustment of learning rates and weight decay parameters has been crucial for enhancing the model's performance. The selection of a

learning rate as a 0.001 and a weight decay of 0.01 has been identified as the best strategy, allowing the models to accurately identify the patterns without overfitting, guaranteeing its relevance and reliability in histopathological images.

5.2 Societal Impact and Contribution to Global Sustainability

Our thesis research focused on the classification of histopathological images pertinent to breast cancer aspires to make a meaningful impact in the biotechnology domain, thereby enhancing the quality of life. The deployment of specific algorithms on histopathological images has been central to our efforts in categorizing cells as a cancer. Our ambition is to be at the forefront of breast cancer diagnosis advancements. The outcomes of our detection and classification endeavors suggest the future feasibility of preliminary reports to medical professionals. The variability in image interpretation, a consequence of human factors, can lead to divergent evaluations, and potentially, erroneous decisions based on the same set of images.

Furthermore, the rising quantity of imaging data is intensifying the already critical shortage of medical resources, underline the urgency of this dilemma. It is anticipated that the outcomes of this research, along with future investigations, will foster the ability to conduct detections with the precision akin to that of a pathologist, thereby allowing these algorithms to be deployed with considerable confidence. This, expectedly, might lighten the load on healthcare providers to a degree. Furthermore, our exploration has been aimed at refining image enhancement methods and fine-tuning algorithmic parameters to discover their most effective setups. The quest for the ideal parameter values is directed not solely at boosting the accuracy in identifying cancer cells but also at improving the clarity of histopathological images. This is important to ensure that the advancements in diagnostic capabilities can be efficiently translated into everyday clinical practice, thereby offering the possibility to greatly enhance patient health outcomes.

The impact of this research stretches beyond mere technical realms, reaching into societal benefits and contributions to global sustainability. An early and precise diagnosis of breast cancer holds a key role in lowering the death rates linked to this disease. By making the diagnostic process more efficient with enhanced algorithms, our investigation

aids in detecting breast cancer earlier, which in turn enables timely and more effective treatments.

Additionally, embracing advanced diagnostic tools matches up with the wider objectives of sustainable healthcare by pushing for resource efficiency and easier access. Better diagnostic tools might lead to a more thoughtful use of medical resources, making sure patients get the most fitting care without the needless overutilization of medical services. This method backs the sustainability of healthcare systems by bettering the distribution of resources and might reduce the environmental impact that comes with providing healthcare.

5.3 Future Prospects

Some suggestions for future work are as follows. Firstly, it should be examined whether better results can be achieved by playing with the parameters of the best algorithms identified in the improvement techniques. Instead of using the entire image as input for enhancement, it might be possible to take coordinates around the cell and apply sharpening to the cell and its surroundings, so each cell could be improved individually. In addition to this, the accuracy of the algorithm could be tested by expanding the dataset through combining it with other histopathological datasets. Besides, by extracting the edge features of the cells in the image and combining them with CNN features, training could be conducted with a more comprehensive feature set.

BIBLIOGRAPHY

[1] R. L. Siegel, K. D. Miller, H. E. Fuchs, and A. Jemal, "Cancer Statistics, 2021.," *CA Cancer J Clin*, vol. 71, no. 1, pp. 7–33, Jan. 2021, doi: 10.3322/caac.21654.

[2] L. Wilkinson and T. Gathani, "Understanding breast cancer as a global health concern.," *Br J Radiol*, vol. 95, no. 1130, p. 20211033, Feb. 2022, doi: 10.1259/bjr.20211033.

[3] M. Yusoff, T. Haryanto, H. Suhartanto, W. A. Mustafa, J. M. Zain, and K. Kusmardi, "Accuracy Analysis of Deep Learning Methods in Breast Cancer Classification: A Structured Review.," *Diagnostics (Basel)*, vol. 13, no. 4, Feb. 2023, doi: 10.3390/diagnostics13040683.

[4] Y. Amethiya, P. Pipariya, S. Patel, and M. Shah, "Comparative analysis of breast cancer detection using machine learning and biosensors," *Intelligent Medicine*, vol. 2, no. 2, pp. 69–81, May 2022, doi: 10.1016/j.imed.2021.08.004.

[5] Y. Hao *et al.*, "Breast cancer histopathological images classification based on deep semantic features and gray level co-occurrence matrix," *PLoS One*, vol. 17, no. 5, p. e0267955, May 2022, doi: 10.1371/journal.pone.0267955.

[6] H. Irshad, A. Veillard, L. Roux, and D. Racoceanu, "Methods for Nuclei Detection, Segmentation, and Classification in Digital Histopathology: A Review—Current Status and Future Potential," *IEEE Rev Biomed Eng*, vol. 7, pp. 97–114, 2014, doi: 10.1109/RBME.2013.2295804.

[7] A. Aksac, D. J. Demetrick, T. Ozyer, and R. Alhajj, "BreCaHAD: a dataset for breast cancer histopathological annotation and diagnosis," *BMC Res Notes*, vol. 12, no. 1, p. 82, Dec. 2019, doi: 10.1186/s13104-019-4121-7.

[8] D. C. Macedo *et al.*, "Evaluating Interpretability in Deep Learning using Breast Cancer Histopathological Images," in *2022 35th SIBGRAPI Conference on Graphics, Patterns and Images (SIBGRAPI)*, IEEE, Oct. 2022, pp. 276–281. doi: 10.1109/SIBGRAPI55357.2022.9991797.

[9] D. Hlavcheva, V. Yaloveha, and A. Podorozhniak, "APPLICATION OF CONVOLUTIONAL NEURAL NETWORK FOR HISTOPATHOLOGICAL ANALYSIS," *Advanced Information Systems*, vol. 3, no. 4, pp. 69–73, Dec. 2019, doi: 10.20998/2522-9052.2019.4.10.

[10] D. P. Bhausaheb and K. L. Kashyap, "Shuffled Shepherd Deer Hunting Optimization based Deep Neural Network for Breast Cancer Classification using Breast Histopathology Images," *Biomed Signal Process Control*, vol. 83, p. 104570, May 2023, doi: 10.1016/j.bspc.2023.104570.

[11] P. Harrison and K. Park, "Tumor Detection In Breast Histopathological Images Using Faster R-CNN," in *2021 International Symposium on Medical Robotics (ISMR)*, IEEE, Nov. 2021, pp. 1–7. doi: 10.1109/ISMR48346.2021.9661483.

[12] M. Zhou, B. Li, and J. Wang, "Optimization of Hyperparameters in Object Detection Models Based on Fractal Loss Function," *Fractal and Fractional*, vol. 6, no. 12, p. 706, Nov. 2022, doi: 10.3390/fractalfract6120706.

[13] S. Cuenat and R. Couturier, “Convolutional Neural Network (CNN) vs Vision Transformer (ViT) for Digital Holography,” in *2022 2nd International Conference on Computer, Control and Robotics (ICCCR)*, IEEE, Mar. 2022, pp. 235–240. doi: 10.1109/ICCCR54399.2022.9790134.
[14] X. Zhou *et al.*, “A Comprehensive Review for Breast Histopathology Image Analysis Using Classical and Deep Neural Networks,” *IEEE Access*, vol. 8, pp. 90931–90956, 2020, doi: 10.1109/ACCESS.2020.2993788.
[15] M. Abdul Jawad and F. Khursheed, “Deep and dense convolutional neural network for multi category classification of magnification specific and magnification independent breast cancer histopathological images,” *Biomed Signal Process Control*, vol. 78, p. 103935, Sep. 2022, doi: 10.1016/j.bspc.2022.103935.
[16] F. A. Spanhol, L. S. Oliveira, C. Petitjean, and L. Heutte, “A Dataset for Breast Cancer Histopathological Image Classification,” *IEEE Trans Biomed Eng*, vol. 63, no. 7, pp. 1455–1462, Jul. 2016, doi: 10.1109/TBME.2015.2496264.
[17] T. H. H. Aldhyani, R. Nair, E. Alzain, H. Alkahtani, and D. Koundal, “Deep Learning Model for the Detection of Real Time Breast Cancer Images Using Improved Dilation-Based Method,” *Diagnostics*, vol. 12, no. 10, p. 2505, Oct. 2022, doi: 10.3390/diagnostics12102505.
[18] A. Sohail, M. A. Mukhtar, A. Khan, M. M. Zafar, A. Zameer, and S. Khan, “Deep Object Detection based Mitosis Analysis in Breast Cancer Histopathological Images,” Mar. 2020.
[19] T. Ilyas, S. Kim, and H. Kim, “Tumor Detection in Breast Histopathology Images via modified Faster-RCNN,” in *Proceedings of the domestic conference of the Control Robot System Society*, ICROS 35th symposium, 2021, pp. 14–17.
[20] H. U. Khan, B. Raza, M. H. Shah, S. M. Usama, P. Tiwari, and S. S. Band, “SMDetector: Small mitotic detector in histopathology images using faster R-CNN with dilated convolutions in backbone model,” *Biomed Signal Process Control*, vol. 81, p. 104414, Mar. 2023, doi: 10.1016/j.bspc.2022.104414.
[21] A. C. Wilson, R. Roelofs, M. Stern, N. Srebro, and B. Recht, “The Marginal Value of Adaptive Gradient Methods in Machine Learning,” May 2017.
[22] J. Chen, D. Zhou, Y. Tang, Z. Yang, Y. Cao, and Q. Gu, “Closing the Generalization Gap of Adaptive Gradient Methods in Training Deep Neural Networks,” Jun. 2018.
[23] L. N. Smith and N. Topin, “Super-Convergence: Very Fast Training of Neural Networks Using Large Learning Rates,” Aug. 2017.
[24] J. Snoek, H. Larochelle, and R. P. Adams, “Practical Bayesian Optimization of Machine Learning Algorithms,” Jun. 2012.
[25] A. Esteva *et al.*, “Dermatologist-level classification of skin cancer with deep neural networks,” *Nature*, vol. 542, no. 7639, pp. 115–118, Feb. 2017, doi: 10.1038/nature21056.
[26] Zuiderveld K, “Contrast limited adaptive histogram equalization,” *Academic Press Professional*, pp. 474–485, 1994.
[27] A. Buades, B. Coll, and J.-M. Morel, “A Non-Local Algorithm for Image Denoising,” in *2005 IEEE Computer Society Conference on Computer*

Vision and Pattern Recognition (CVPR'05), IEEE, 2005, pp. 60–65. doi: 10.1109/CVPR.2005.38.
[28] S. M. Pizer, R. E. Johnston, J. P. Ericksen, B. C. Yankaskas, and K. E. Muller, "Contrast-limited adaptive histogram equalization: speed and effectiveness," in *[1990] Proceedings of the First Conference on Visualization in Biomedical Computing*, IEEE Comput. Soc. Press, 1990, pp. 337–345. doi: 10.1109/VBC.1990.109340.
[29] Rafael C. Gonzalez, *Digital Image Processing*, 2nd ed. Prentice-Hall Of India Pvt. Limited, 2002.
[30] P. Burt and E. Adelson, "The Laplacian Pyramid as a Compact Image Code," *IEEE Transactions on Communications*, vol. 31, no. 4, pp. 532–540, Apr. 1983, doi: 10.1109/TCOM.1983.1095851.
[31] A. R. Smith, "Color gamut transform pairs," *ACM SIGGRAPH Computer Graphics*, vol. 12, no. 3, pp. 12–19, Aug. 1978, doi: 10.1145/965139.807361.
[32] R. Girshick, J. Donahue, T. Darrell, and J. Malik, "Rich feature hierarchies for accurate object detection and semantic segmentation," Nov. 2013.
[33] R. Girshick, "Fast R-CNN," in *2015 IEEE International Conference on Computer Vision (ICCV)*, IEEE, Dec. 2015, pp. 1440–1448. doi: 10.1109/ICCV.2015.169.
[34] S. Ren, K. He, R. Girshick, and J. Sun, "Faster R-CNN: Towards Real-Time Object Detection with Region Proposal Networks," Jun. 2015.
[35] T.-Y. Lin *et al.*, "Microsoft COCO: Common Objects in Context," 2014, pp. 740–755. doi: 10.1007/978-3-319-10602-1_48.
[36] K. He, X. Zhang, S. Ren, and J. Sun, "Deep Residual Learning for Image Recognition," Dec. 2015.
[37] T.-Y. Lin, P. Dollar, R. Girshick, K. He, B. Hariharan, and S. Belongie, "Feature Pyramid Networks for Object Detection," in *2017 IEEE Conference on Computer Vision and Pattern Recognition (CVPR)*, IEEE, Jul. 2017, pp. 936–944. doi: 10.1109/CVPR.2017.106.
[38] A. Howard *et al.*, "Searching for MobileNetV3," in *2019 IEEE/CVF International Conference on Computer Vision (ICCV)*, IEEE, Oct. 2019, pp. 1314–1324. doi: 10.1109/ICCV.2019.00140.
[39] L. Bottou, "Large-Scale Machine Learning with Stochastic Gradient Descent," in *Proceedings of COMPSTAT'2010*, Heidelberg: Physica-Verlag HD, 2010, pp. 177–186. doi: 10.1007/978-3-7908-2604-3_16.
[40] D. P. Kingma and J. Ba, "Adam: A Method for Stochastic Optimization," Dec. 2014.
[41] I. Loshchilov and F. Hutter, "Decoupled Weight Decay Regularization," Nov. 2017.
[42] Tijmen Tieleman and G. Hinton, "Lecture 6.5-rmsprop: Divide the gradient by a running average of its recent magnitude," *COURSERA: Neural networks for machine learning*, vol. 4, no. 2, pp. 26–31, 2012.
[43] L. N. Smith and N. Topin, "Super-Convergence: Very Fast Training of Neural Networks Using Large Learning Rates," Aug. 2017.
[44] BrecaHad, "BreCa_v5 Dataset," Roboflow Universe. Accessed: Mar. 03, 2024. [Online]. Available: https://universe.roboflow.com/brecahad/breca_v5
[45] I. Kandel and M. Castelli, "The effect of batch size on the generalizability of the convolutional neural networks on a histopathology dataset," *ICT*

Express, vol. 6, no. 4, pp. 312–315, Dec. 2020, doi: 10.1016/j.icte.2020.04.010.

[46] H. Rezatofighi, N. Tsoi, J. Gwak, A. Sadeghian, I. Reid, and S. Savarese, "Generalized Intersection Over Union: A Metric and a Loss for Bounding Box Regression," in *2019 IEEE/CVF Conference on Computer Vision and Pattern Recognition (CVPR)*, IEEE, Jun. 2019, pp. 658–666. doi: 10.1109/CVPR.2019.00075.

[47] J. Davis and M. Goadrich, "The relationship between Precision-Recall and ROC curves," in *Proceedings of the 23rd international conference on Machine learning - ICML '06*, New York, New York, USA: ACM Press, 2006, pp. 233–240. doi: 10.1145/1143844.1143874.

[48] D. C. Blair, "Information Retrieval, 2nd ed. C.J. Van Rijsbergen. London: Butterworths; 1979: 208 pp. Price: $32.50," *Journal of the American Society for Information Science*, vol. 30, no. 6, pp. 374–375, Nov. 1979, doi: 10.1002/asi.4630300621.

[49] A. Krogh and J. A. Hertz, "A Simple Weight Decay Can Improve Generalization," *Neural Information Processing Systems*, pp. 950–957, 1991.

CURRICULUM VITAE

2009 – 2014	B.Sc., Computer Engineering, Meliksah University, Kayseri, TURKEY
2010 – 2014	B.Sc., Business Administration, Meliksah University, Kayseri, TURKEY
2019 – Present	M.Sc., Electrical and Computer Engineering, Abdullah Gul University, Kayseri, TURKEY